Improved quasiparticle wave functions and mean field for G_0W_0 calculations: Initialization with the COHSEX operator

Manish Jain,[1,2,3,4] Jack Deslippe,[2,3,5] Georgy Samsonidze,[2,3,*] Marvin L. Cohen,[2,3]
James R. Chelikowsky,[1,6] and Steven G. Louie[2,3]

[1]*Center for Computational Materials, Institute for Computational Engineering and Sciences, University of Texas, Austin, Texas 78712, USA*
[2]*Department of Physics, University of California at Berkeley, Berkeley, California 94720, USA*
[3]*Materials Sciences Division, Lawrence Berkeley National Laboratory, Berkeley, California 94720, USA*
[4]*Department of Physics, Indian Institute of Science, Bangalore 560 012, India*
[5]*NERSC, Lawrence Berkeley National Laboratory, Berkeley, California 94720, USA*
[6]*Departments of Physics and Chemical Engineering, University of Texas, Austin, Texas 78712, USA*

(Received 11 September 2013; revised manuscript received 25 July 2014; published 26 September 2014)

The GW approximation to the electron self-energy has become a standard method for *ab initio* calculation of excited-state properties of condensed-matter systems. In many calculations, the GW self-energy operator, Σ, is taken to be diagonal in the density functional theory (DFT) Kohn-Sham basis within the G_0W_0 scheme. However, there are known situations in which this diagonal G_0W_0 approximation starting from DFT is inadequate. We present two schemes to resolve such problems. The first, which we called sc-COHSEX+GW, involves construction of an improved mean field using the static limit of GW, known as COHSEX (Coulomb hole and screened exchange), which is significantly simpler to treat than GW. In this scheme, frequency-dependent self energy $\Sigma(\omega)$, is constructed and taken to be diagonal in the COHSEX orbitals after the system is solved self-consistently within this formalism. The second method is called off diagonal-COHSEX GW (od-COHSEX+GW). In this method, one does not self-consistently change the mean-field starting point but diagonalizes the COHSEX Hamiltonian within the Kohn-Sham basis to obtain quasiparticle wave functions and uses the resulting orbitals to construct the GW Σ in the diagonal form. We apply both methods to a molecular system, silane, and to two bulk systems, Si and Ge under pressure. For silane, both methods give good quasiparticle wave functions and energies. Both methods give good band gaps for bulk silicon and maintain good agreement with experiment. Further, the sc-COHSEX+GW method solves the qualitatively incorrect DFT mean-field starting point (having a band overlap) in bulk Ge under pressure.

DOI: 10.1103/PhysRevB.90.115148 PACS number(s): 71.15.Qe

I. INTRODUCTION

The GW approximation to the electron self-energy has become the method of choice for treating the electronic excited-state properties of materials from first principles [1–3]. This approach, typically implemented starting from a density functional theory (DFT) mean field, has been shown to work extremely well for a wide variety of condensed-matter systems—metals [4], semiconductors and insulators [2,3], and nanostructures [5]. However, there are a few cases in which some of the common approximations used in most *ab initio* GW calculations are inadequate.

While in most cases approximate Kohn-Sham DFT band structures provide an excellent starting point for GW calculations, in some cases they predict a qualitatively incorrect initial band structure. Some notable cases of this failure are in the strongly correlated systems, such as Mott insulators [6,7]. However, sometimes incorrect ordering of bands can occur even in simple semiconductor systems such as bulk Ge [8].

Another commonly used approximation in *ab initio* GW calculations is that the DFT wave functions are the same as the quasiparticle wave functions. Some examples in which this approximation may break down occur in the calculation of electron affinity in molecular systems and defect levels in solids. For instance, in molecular systems, quasiparticle states of interest could have a mean-field energy level below the vacuum level, whereas the actual quasiparticle level (after the self-energy correction) may be above the vacuum level. The former is a localized bound state; the latter is a resonant state [9]. A similar problem can occur with defect states in solids. The defect level within DFT (because of band-gap underestimation) can be within the conduction-band continuum (a resonant state), however after the GW self-energy correction, the level is within the band gap of the solid (a localized state) [10].

Several attempts have been made to address the mean-field starting band structure for GW [6,11–16]. For strongly correlated systems, the LDA+U (local density approximation + on-site Hubbard interaction) method has become the method of choice. This method has been shown to work well for systems containing *d*- and *f*-shell electrons [6,15]. However, the method requires selecting a proper Hubbard "U." Recently, some progress has been made in calculating this "U" from *ab initio* methods [15,17,18]. However, this method is not useful in simple semiconductors such as bulk Ge under pressure. Going beyond the Kohn-Sham formulation of DFT [19]—the generalized Kohn-Sham (GKS) DFT has been used to construct a different starting mean field [14,16]. While there are some attempts to make GKS more reliable in predicting accurate electronic structures [20,21], the most commonly used GKS functionals give varying results [22]. Existing GKS formulations offer a different starting point, but it is

*Present address: Research and Technology Center, Robert Bosch LLC, Cambridge, MA 02142, USA.

not clear *a priori* whether it is better. In some cases, it has been shown to be a better mean field, while in other cases not so [16,23]. Another method is the QPscGW approach of Faleev *et al.* [11] that iteratively produces a mean-field starting point such that, by construction, the quasiparticle wave functions and mean-field orbitals are close. This approach is conceptually elegant; however, as we discuss below, this approach has a very high computational cost.

Alternatively, several groups [12,13] have constructed a frequency-independent Hamiltonian in the so called COHSEX (Coulomb hole and screened exchange) approximation and carried out the calculation using Kohn-Sham DFT orbitals as a basis to varying levels of self-consistency for a mean-field starting point for a subsequent GW calculation. While in principle the COHSEX offers a good mean-field starting point, in practice using Kohn-Sham orbitals as a basis makes the current schemes cumbersome, as discussed below.

Most current solutions to this issue involve expanding the quasiparticle wave functions in terms of the mean-field orbitals [24]. Subsequently, the off-diagonal elements of Σ are calculated on a grid of frequencies. This is conceptually and numerically difficult. It is also not clear *a priori* how many states should be included in the expansion. Further, the off-diagonal matrix elements of the GW Hamiltonian in the Kohn-Sham basis can sometimes converge slowly with respect to the Hamiltonian matrix size. As a result, one can obtain results that suffer due to a small basis set used for constructing the Hamiltonian matrix—whether it be the GW [13,24] or COHSEX [12] or the QPscGW [11] Hamiltonian.

In this paper, we present two alternative methods based on the COHSEX approximation starting point. These methods allow us to efficiently construct both an improved mean field and quasiparticle wave functions without the shortcomings of the above-mentioned methods. The first method is a fully self-consistent COHSEX followed by GW (sc-COHSEX+GW) method, where a new mean field and approximate quasiparticle wave functions are obtained from a self-consistent solution to the COHSEX Hamiltonian. The second, the off-diagonal COHSEX followed by GW (od-COHSEX+GW) method, allows for a computationally less intensive treatment of effectively using just the off-diagonal matrix elements (in the Kohn-Sham basis) within a one-shot COHSEX Hamiltonian to obtain the approximate quasiparticle wave functions. Both approaches have been implemented within a plane-wave basis set. The main advantage of these methods over previous ones is that our methods are conceptually simple, transparent, and one can work completely in a plane-wave basis. Despite a much more complete basis set than the limited number of Kohn-Sham orbitals traditionally used, these methods are computationally efficient. Both approaches do not require an explicit construction of the Hamiltonian. As in typical DFT calculations, only the Hamiltonian times the wave function is required. We apply these methods to the molecular example of silane and bulk solid examples of silicon and germanium under pressure. These methods make a significant improvement to the electron affinity of silane and a better and well-defined starting mean field for Ge under pressure. In silicon, the od-COHSEX+GW gives virtually identical quasiparticle energies to a conventional G_0W_0 calculation. The sc-COHSEX+GW, on the other hand, as expected overestimates the band gaps for reasons to be discussed below.

II. METHODS

Current state-of-the-art *ab initio* calculation of quasiparticle energies (i.e., the one-particle excitations) of real materials is based on the GW approximation to the electron self-energy. Within the many-body Green's-function formalism, quasiparticle energies and wave functions can be obtained by solving the Dyson equation [1,2]:

$$\left[-\frac{1}{2}\nabla^2 + V_{\rm ion}(\mathbf{r}) + V_{\rm H}(\mathbf{r})\right]\psi^{\rm QP}(\mathbf{r}) + \int \Sigma(\mathbf{r},\mathbf{r}',E^{\rm QP})\psi^{\rm QP}(\mathbf{r}')d\mathbf{r}' = E^{\rm QP}\psi^{\rm QP}(\mathbf{r}), \quad (1)$$

where $V_{\rm ion}(\mathbf{r})$ is the ionic potential, $V_{\rm H}(\mathbf{r})$ is the Hartree potential, Σ is the self-energy operator within the GW approximation, and $E^{\rm QP}$ and $\psi^{\rm QP}$ are the quasiparticle energies and wave functions, respectively. The self-energy operator is a nonlocal frequency-dependent operator that incorporates the many-electron effects. It should be noted that Eq. (1) is not a Hermitian eigenvalue problem. The eigenvalues, $E^{\rm QP}$, are complex with the imaginary part related to the quasiparticle lifetime. To solve Eq. (1), the dynamic Σ needs to be evaluated at $E^{\rm QP}$ in a self-consistent way.

Solving Eq. (1) is challenging as the self-energy operator is a functional of the many-body Green's function. Typically, instead of solving Eq. (1), the quasiparticle energies are calculated within a first-order perturbation theory approximation starting from a mean-field calculation [2,3]. As we noted in the Introduction, DFT in the Kohn-Sham formulation is often chosen as the starting point for GW calculation. Further, the self-energy operator is constructed using the mean field G and W, called the G_0W_0 approximation. We use the notation, $\Sigma_{GW}(\{E^{\rm DFT},\psi^{\rm DFT},\varepsilon^{-1}_{\rm DFT}\};E^{\rm QP})$, to indicate that the self-energy, $\Sigma(\mathbf{r},\mathbf{r}',E)$, is constructed using DFT eigenvalues, $E^{\rm DFT}$, eigenfunctions, $\psi^{\rm DFT}$, and dielectric matrix, $\varepsilon^{-1}_{\rm DFT}$, and evaluated at the quasiparticle energy, $E^{\rm QP}$. When the quasiparticle energies are calculated as

$$E^{\rm QP} = E^{\rm DFT} + \langle\psi^{\rm DFT}|\Sigma_{GW}\left(\left\{E^{\rm DFT},\psi^{\rm DFT},\varepsilon^{-1}_{\rm DFT}\right\};E^{\rm QP}\right) - V_{\rm XC}|\psi^{\rm DFT}\rangle, \quad (2)$$

it is called the *diagonal* G_0W_0 approximation. In Eq. (2), $V_{\rm XC}$ is the exchange-correlation potential within DFT and the self-energy Σ_{GW} is evaluated self-consistently at the quasiparticle energy $E^{\rm QP}$. The DFT eigenvalues, eigenfunctions, and exchange-correlation potential are obtained by solving the self-consistent Kohn-Sham equations:

$$\left[-\tfrac{1}{2}\nabla^2 + V_{\rm ion}(\mathbf{r}) + V_{\rm H}(\mathbf{r}) + V_{\rm XC}(\mathbf{r})\right]\psi^{\rm DFT}(\mathbf{r}) = E^{\rm DFT}\psi^{\rm DFT}(\mathbf{r}), \quad (3)$$

where $V_{\rm XC}(\mathbf{r})$ is constructed within a suitable approximation—common approximations being the local density approximation (LDA) [25] and the generalized-gradient approximation (GGA) [26]. As seen from Eq. (2), the diagonal G_0W_0 approach assumes that the DFT mean-field solutions (often LDA or GGA) are a good starting point. It also assumes

that DFT eigenfunctions are a good approximation to the quasiparticle wave functions. These assumptions are valid for many bulk materials and nanostructures, as discussed in Ref. [2]. However, as discussed previously, there are known limitations of these approximations in specific cases.

Let us first discuss the case in which $\psi^{\mathrm{QP}} \not\approx \psi^{\mathrm{DFT}}$. As we noted in the Introduction, the current method to address this problem is to diagonalize the full G_0W_0 matrix [13,24,27], $H_{ij} = E^{\mathrm{DFT}}\delta_{ij} + \langle\psi_i^{\mathrm{DFT}}|\Sigma_{GW}(\{E^{\mathrm{DFT}},\psi^{\mathrm{DFT}},\varepsilon_{\mathrm{DFT}}^{-1}\};E^{\mathrm{QP}}) - \mathrm{V_{XC}}|\psi_j^{\mathrm{DFT}}\rangle$, constructed in the DFT eigenfunction basis ψ_i^{DFT}. While in principle all DFT eigenstates should be used in the expansion, in practice, due to the cost of constructing the off-diagonal matrix elements, $\langle\psi_i^{\mathrm{DFT}}|\Sigma_{GW}(\{E^{\mathrm{DFT}},\psi^{\mathrm{DFT}},\varepsilon_{\mathrm{DFT}}^{-1}\};E^{\mathrm{QP}})|\psi_j^{\mathrm{DFT}}\rangle$, the matrix is limited to a small number of DFT basis states (rows/columns). *A priori*, it is not obvious how many DFT wave functions should be used in the expansion. All the matrix elements of the self-energy operator do not contribute equally to the self-energy of the state of interest. As a result, there can be several states with a small contribution followed by a state with a large contribution. This makes checking for convergence cumbersome. Additionally, all the matrix elements should in principle be evaluated at E^{QP} for each separate quasiparticle level, which is challenging to evaluate in a self-consistent fashion. Thus, diagonalizing the full G_0W_0 matrix with sufficient rows and columns and appropriate energy dependence is extremely difficult.

Instead of constructing and diagonalizing the full G_0W_0 matrix in the ψ^{DFT} basis, we propose the od-COHSEX+GW approach as shown on the left side of Fig. 1. In this approach, using the DFT eigenvalues and eigenfunctions, we construct the COHSEX operator *in a plane-wave basis set* up to the convergent plane-wave DFT wave-function cutoff. In particular, in the COHSEX operator, the screened exchange (SEX) and Coulomb hole (COH) terms, which are computed from the DFT eigenfunctions and eigenvalues, are expressed as matrices in the plane-wave basis. We then diagonalize the COHSEX Hamiltonian, $(H_0^{\mathrm{DFT}} + \Sigma_{\mathrm{COHSEX}})$, using an iterative algorithm such as the Lanczos algorithm. Here H_0^{DFT} is defined as the DFT Hamiltonian, shown in Eq. (3), without the exchange-correlation term, V_{XC}. It is worthwhile to point out that solving this eigensystem iteratively only requires one to compute $(H_0^{\mathrm{DFT}} + \Sigma_{\mathrm{COHSEX}})\psi$ products, where ψ is some trial quasiparticle wave function. In the next sections, we provide the exact expressions and computational complexity for evaluating $\Sigma_{\mathrm{COHSEX}}\psi$ within the plane-wave basis set.

After solving this eigensystem, one then does a diagonal G_0W_0 calculation as shown on the left side of Fig. 1, but now in the basis of the od-COHSEX quasiparticle wave functions, called the od-COHSEX+GW approach. This approach, which is equivalent to diagonalizing the G_0W_0 matrix in the static limit in a complete plane-wave basis, is an effective scheme for the inclusion of the off-diagonal G_0W_0 matrix elements in the Kohn-Sham basis. It can also be seen as a transformation to a basis within which the G_0W_0 matrix (still constructed from G_0 and W_0 using the DFT eigenvalues and eigenfunctions) is nearly diagonal.

For the problem related to the starting mean-field band structure, we propose the self-consistent COHSEX method. Here one could replace the DFT mean-field starting solutions completely by replacing the DFT mean-field Hamiltonian with a self-consistent COHSEX (sc-COHSEX) mean-field Hamiltonian. This approach is outlined on the right side of Fig. 1. As before, we use the DFT eigenfunctions and eigenvalues to construct an initial polarizability and dielectric matrix. However, in this second approach, the COHSEX operator is updated self-consistently as we diagonalize the COHSEX Hamiltonian. The eigenvalues and eigenfunctions from this diagonalization are used to construct a new polarizability and dielectric matrix. This process is repeated to reach self-consistency in the dielectric matrix. In practice, for the systems considered, we find that one/two updates of the polarizability are sufficient. We then do a standard diagonal G_0W_0 calculation, in the basis of the sc-COHSEX orbitals, using the sc-COHSEX eigenvalues, eigenfunctions, and updated polarizability as our mean-field starting point. This is the sc-COHSEX+GW approach.

We now compare our sc-COHSEX method with previous self-consistent quasiparticle methods of Bruneval *et al.* [12] and QPscGW [11]. In the work of Bruneval *et al.* [12], a similar self-consistent COHSEX approach is used, with the important difference that they work in the DFT Kohn-Sham orbital basis.

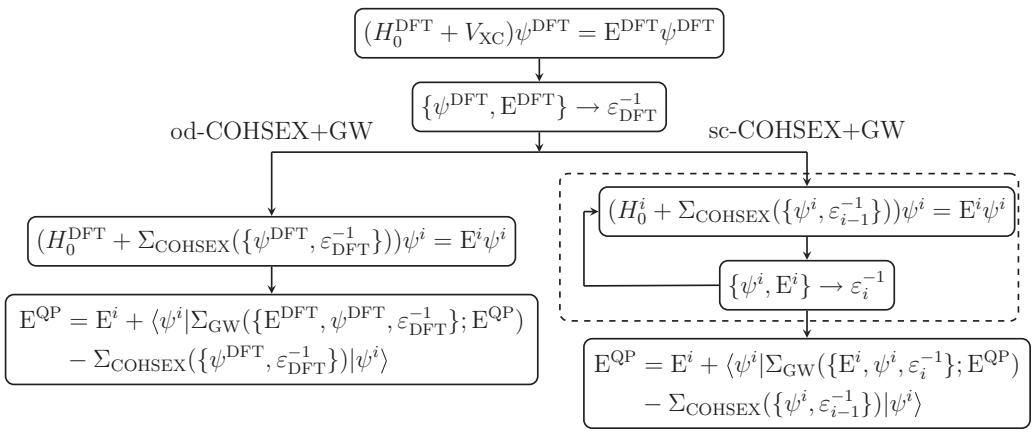

FIG. 1. Outline of the od-COHSEX+GW and the sc-COHSEX+GW methodologies. The H_0^i refers to the kinetic, ionic, and Hartree potentials constructed with density from ψ^i. See text for details.

In particular, they construct the off-diagonal matrix elements of the COHSEX operator using only valence-band and low-energy conduction-band states. This restricts the degrees of freedom that the quasiparticle wave functions have. We avoid this problem by working directly in a plane-wave basis with a large cutoff to construct and diagonalize the sc-COHSEX Hamiltonian operator. Using this complete basis removes any bias on the low-energy orbitals, and more importantly on the dielectric matrix. The QPscGW approach [11] does not make use of the COHSEX approximation. It seeks a mean field that gives eigenvalues closest to the quasiparticle energies iteratively. However, the QPscGW approach also suffers from the same problem of working in a restricted basis as formulated in Ref. [12]. In this case, the restricted basis is required due to the extremely high computational costs of constructing the Σ matrix that includes some dynamical effects, because one must sum over a large number of empty states as well as integrate over frequencies when constructing each matrix element of Σ. Additionally, this method (as well as the sc-COHSEX+GW methods described above) tends to overestimate band gaps because the gap in the self-consistent mean field used to construct the random-phase approximation (RPA) polarizability is higher than the optical gap of the system. It is well known [28,29] that self-consistency in the RPA polarizability would be canceled by vertex (or excitonic) effects in the final dielectric response, and so including only self-consistency without higher-order corrections leads to too large gaps. The od-COHSEX+GW approach, on the other hand, does not suffer from this problem. In the od-COHSEX+GW approach, we continue to use the DFT (LDA or GGA) RPA polarizability and Σ, but we account for the fact that the quasiparticle wave functions may no longer be the Kohn-Sham orbitals.

III. IMPLEMENTATION IN A BASIS OF PLANE WAVES

We describe here our plane-wave implementation of the methods developed in Sec. II. In applying the Hamiltonian, $(H_0^i + \Sigma_{\mathrm{COHSEX}})$, to an arbitrary wave function, ψ, only the $\Sigma_{\mathrm{COHSEX}}\psi$ products are different from their corresponding DFT counterparts. In this section, we only give details of the implementation of these new products. We adopt the following convention for the Fourier transformation from real to reciprocal space. The wave function $\psi_{n,\mathbf{k}}(\mathbf{r})$ of band n at Bloch wave vector $\mathbf{k}$ transforms according to

$$\psi_{n,\mathbf{k}}(\mathbf{r}) = \frac{1}{\sqrt{\Omega}} \sum_{\mathbf{G}} e^{i(\mathbf{k}+\mathbf{G})\cdot\mathbf{r}} u_{n,\mathbf{k}}(\mathbf{G}), \tag{4}$$

where Ω is the volume of the unit cell and $u_{n,\mathbf{k}}(\mathbf{G})$ is the Fourier transform of the cell periodic part of the wave function, $u_{n,\mathbf{k}}(\mathbf{r})$. For spin-unpolarized systems, the screened exchange operator, Σ_{SEX}, within the COHSEX approximation is given as [1,2]

$$\Sigma_{\mathrm{SEX}}(\mathbf{r},\mathbf{r}') = -\frac{1}{N_{\mathbf{k}}} \sum_{n,\mathbf{k}}^{\mathrm{occ.}} \psi_{n,\mathbf{k}}(\mathbf{r})\psi^*_{n,\mathbf{k}}(\mathbf{r}')W(\mathbf{r},\mathbf{r}') \tag{5}$$

$$= -\frac{1}{2N_{\mathbf{k}}} \sum_{n,\mathbf{k}} f_{n,\mathbf{k}}\psi_{n,\mathbf{k}}(\mathbf{r})\psi^*_{n,\mathbf{k}}(\mathbf{r}')W(\mathbf{r},\mathbf{r}'), \tag{6}$$

where $W(\mathbf{r},\mathbf{r}')$ is the screened Coulomb interaction at frequency, $\omega = 0$, $N_{\mathbf{k}}$ is the number of Bloch vectors $\mathbf{k}$ in the discretized Brillouin zone, and $f_{n,\mathbf{k}} = \{2 \text{ if occupied}, 0 \text{ if unoccupied}\}$ is the occupation of band n with wave vector $\mathbf{k}$. The screened Coulomb interaction is given in terms of the bare Coulomb interaction $v(\mathbf{r},\mathbf{r}')$ as

$$W(\mathbf{r},\mathbf{r}') = \int d\mathbf{r}'' \varepsilon^{-1}(\mathbf{r},\mathbf{r}'')v(\mathbf{r}'',\mathbf{r}') \tag{7}$$

$$= \sum_{\mathbf{q},\mathbf{G},\mathbf{G}'} e^{i(\mathbf{q}+\mathbf{G})\cdot\mathbf{r}} W_{\mathbf{q}}(\mathbf{G},\mathbf{G}') e^{-i(\mathbf{q}+\mathbf{G}')\cdot\mathbf{r}'} \tag{8}$$

$$= \sum_{\mathbf{q},\mathbf{G},\mathbf{G}'} e^{i(\mathbf{q}+\mathbf{G})\cdot\mathbf{r}} \varepsilon^{-1}_{\mathbf{q}}(\mathbf{G},\mathbf{G}') v_{\mathbf{q}}(\mathbf{G}') e^{-i(\mathbf{q}+\mathbf{G}')\cdot\mathbf{r}'}, \tag{9}$$

where $\varepsilon^{-1}(\mathbf{r}'',\mathbf{r}')$ is the static RPA dielectric matrix, $\mathbf{q}$ is a Bloch wave vector and $\varepsilon^{-1}_{\mathbf{q}}(\mathbf{G},\mathbf{G}')$ and $v_{\mathbf{q}}(\mathbf{G}')$ are the Fourier transforms of the dielectric matrix and bare Coulomb interaction, respectively, defined analogously to Eq. (8). The action of the screened exchange operator on a wave function of band m at wave vector $\mathbf{q}$, $\psi_{m,\mathbf{q}}(\mathbf{r})$, can be written as

$$\int_{\Omega_s} d\mathbf{r}' \Sigma_{\mathrm{SEX}}(\mathbf{r},\mathbf{r}')\psi_{m,\mathbf{q}}(\mathbf{r}')$$

$$= -\frac{1}{2N_{\mathbf{k}}} \sum_{n,\mathbf{k}} f_{n,\mathbf{k}}\psi_{n,\mathbf{k}}(\mathbf{r}) \sum_{\mathbf{G}} e^{-i(\mathbf{q}-\mathbf{k}+\mathbf{G})\cdot\mathbf{r}}$$

$$\times \sum_{\mathbf{G}'} Y_{n,\mathbf{k},m,\mathbf{q}}(\mathbf{G}')\varepsilon^{-1}_{\mathbf{q}-\mathbf{k}}(\mathbf{G},\mathbf{G}')v_{\mathbf{q}-\mathbf{k}}(\mathbf{G}'), \tag{10}$$

where Ω_s is the volume of the entire crystal and $Y_{n,\mathbf{k},m,\mathbf{q}}(\mathbf{G}')$ is the Fourier transform of the codensity:

$$\psi^*_{n,\mathbf{k}}(\mathbf{r})\psi_{m,\mathbf{q}}(\mathbf{r}) = \frac{1}{\Omega} \sum_{\mathbf{G}} Y_{n,\mathbf{k},m,\mathbf{q}}(\mathbf{G}) e^{i(\mathbf{q}-\mathbf{k}+\mathbf{G})\cdot\mathbf{r}}. \tag{11}$$

Similarly, the Coulomb hole operator in the COHSEX, Σ_{COH}, can be expressed in terms of the screened and bare Coulomb interactions as

$$\Sigma_{\mathrm{COH}}(\mathbf{r},\mathbf{r}') = \tfrac{1}{2}[W(\mathbf{r},\mathbf{r}') - v(\mathbf{r},\mathbf{r}')]\delta(\mathbf{r}-\mathbf{r}'). \tag{12}$$

The application of the Σ_{COH} operator on a wave function of band m at wave vector $\mathbf{q}$, $\psi_{m,\mathbf{q}}(\mathbf{r})$, can be written as

$$\int_{\Omega_s} d\mathbf{r}' \Sigma_{\mathrm{COH}}(\mathbf{r},\mathbf{r}')\psi_{m,\mathbf{q}}(\mathbf{r}') \equiv V_{\mathrm{COH}}(\mathbf{r})\psi_{m,\mathbf{q}}(\mathbf{r}), \tag{13}$$

where $V_{\mathrm{COH}}(\mathbf{r})$ is a local, cell-periodic potential whose Fourier transform $V_{\mathrm{COH}}(\mathbf{G})$ is given as

$$V_{\mathrm{COH}}(\mathbf{G}) = \int_{\Omega} d\mathbf{r}\, V_{\mathrm{COH}}(\mathbf{r}) e^{-i\mathbf{G}\cdot\mathbf{r}} \tag{14}$$

$$= \frac{1}{2} \sum_{\mathbf{q},\mathbf{G}'} \left[\varepsilon^{-1}_{\mathbf{q}}(\mathbf{G}+\mathbf{G}',\mathbf{G}') - \delta_{\mathbf{G},0}\right] v_{\mathbf{q}}(\mathbf{G}'). \tag{15}$$

Using Eqs. (10) and (15), Σ_{COHSEX} can be applied to any wave function in the Brillouin zone. We note that the difference in the od-COHSEX+GW approach and the sc-COHSEX+GW approach is only in the wave functions and dielectric matrices used to construct the operator. If one takes the screened Coulomb operator to be the bare Coulomb operator (i.e.,

$\varepsilon^{-1} = 1$), then the above expressions reduce to the Hartree-Fock expressions. Equations (10) and (15) can be easily implemented within any code that performs GKS calculations. The above expressions can be further reduced based on symmetries, as shown in Appendix A.

IV. COMPUTATIONAL COMPLEXITY

Here we analyze the scaling properties of the algorithms proposed in Sec. III. For the purpose of this analysis, we consider only a Γ-point sampling of the Brillouin zone. We assume that the mean-field wave functions are expanded in a basis of plane waves with a kinetic-energy cutoff $E_{\rm cut}^{\rm wf}$. We restrict our analysis for the case of norm-conserving pseudopotentials where the charge density can be expanded in a basis of plane waves with a cutoff $E_{\rm cut}^{\rm den} = 4E_{\rm cut}^{\rm wf}$ corresponding to $N_{\mathbf{G}}^{\rm den}$ plane waves and $N_{\mathbf{r}}^{\rm den}$ grid points in real space. The screened Coulomb interaction is described by a smaller cutoff $E_{\rm cut}^{s}$ corresponding to $N_{\mathbf{G}}^{s}$ plane waves.

The calculation of the codensity [Eq. (11)] can be performed using fast Fourier transforms (FFT) and requires $N_{\rm FFT}^{\rm den} = N_{\mathbf{r}}^{\rm den} \ln(N_{\mathbf{r}}^{\rm den})$ floating point operations. As a result, the application of $\Sigma_{\rm SEX}$ to a wave function as given in Eq. (10) requires $N_v[(N_{\mathbf{G}}^{s})^2 + N_{\mathbf{G}}^{\rm den} + N_{\rm FFT}^{\rm den}]$ floating point operations, where N_v is the number of occupied states. The first term in this expression for the number of floating point operations, $N_v(N_{\mathbf{G}}^{s})^2$, comes from the sum over $\mathbf{G}$ and $\mathbf{G}'$ up to $E_{\rm cut}^{s}$ in Eq. (10). The second term is a result of the diagonal approximation of $\varepsilon_{\mathbf{q}}^{-1}(\mathbf{G},\mathbf{G}')$ beyond the $E_{\rm cut}^{s}$ until the $E_{\rm cut}^{\rm den}$. This diagonal approximation leads to just a sum over $\mathbf{G}$ in Eq. (10). The third term is due to the calculation of the codensity.

The construction of the $V_{\rm COH}(\mathbf{r})$ operator in Eq. (15) only requires $(N_{\mathbf{G}}^{s})^2 + N_{\rm FFT}^{\rm den}$ floating point operations. Its application to a wave function [Eq. (13)] can be done in $N_{\rm FFT}^{\rm den}$ floating point operations. If the size of Krylov subspace required for iterative diagonalization is $N_{\rm Krylov}$, then the floating point operations required for determining a mean-field wave function within od-COHSEX approach would be

$$N_{\rm flops}^{\text{od-COHSEX}} = N_{\rm Krylov}\left\{N_v\left[\left(N_{\mathbf{G}}^{s}\right)^2 + N_{\mathbf{G}}^{\rm den} + N_{\rm FFT}^{\rm den}\right] + N_{\rm FFT}^{\rm den}\right\} + \left(N_{\mathbf{G}}^{s}\right)^2 + N_{\rm FFT}^{\rm den}.$$

As $N_{\mathbf{G}}^{s}$, $N_{\mathbf{r}}^{\rm den}$, $N_{\mathbf{G}}^{\rm den}$, and N_v scale linearly with the size of the system as measured by the number of atoms $N_{\rm at}$, the overall scaling of this calculation is $N_{\rm at}^3$. The number of floating point operations for application of Σ to determine the mean-field wave functions in the sc-COHSEX approach (for a given ε) is $N_v N_{\rm flops}^{\text{od-COHSEX}}$. This is because in the sc-COHSEX approach, all the occupied wave functions have to be computed. Furthermore, one would recalculate a new ε_i^{-1} in each iteration (as described in Fig. 1). Overall, this would make the scaling of the calculation $N_{\rm at}^4$.

It is also worthwhile to consider the scaling of the traditional methods, where the quasiparticle wave function is expanded in terms of N_b mean-field wave functions. In these approximations, if the off-diagonal Σ matrix elements are included in the static limit, the cost of evaluating each Σ matrix element remains the same as $N_{\rm flops}^{\text{od-COHSEX}}$. However, as the number of wave functions is N_b, the total cost is $N_b N_{\rm flops}^{\text{od-COHSEX}}$. It must be pointed out that N_b also scales linearly with the size of the system, $N_{\rm at}$. This is because as the size of the system increases, the number of wave functions in a fixed energy range also increases, which would lead to the best-case scaling of $N_{\rm at}^4$. For the self-consistent calculation, the scaling behavior would remain the same. If the off-diagonal matrix elements include frequency effects, the number of floating point operations needed also get multiplied by a factor related to the integration in the frequency domain. Thus, despite working in a nearly complete plane-wave basis, the od-COHSEX and sc-COHSEX approaches are more efficient compared to the traditional approaches to the problem.

V. RESULTS AND DISCUSSION

To illustrate the application of our methods, we examine the silane molecule. It has been shown [13,27] that the Kohn-Sham LUMO level is below the vacuum level in DFT, but the physical LUMO quasiparticle energy is above the vacuum level, i.e., the molecule possesses a negative electron affinity. This leads to a qualitative difference in the spatial extent of the DFT and quasiparticle wave function—the Kohn-Sham wave function is localized, while the quasiparticle one mixes with the continuum states and is a resonant state.

Our DFT calculations were performed using plane waves and pseudopotentials in a supercell geometry [30] as implemented in PARATEC [31]. We expanded the wave functions in plane waves up to an energy cutoff of 75 Ry. We used the Γ-point sampling of the Brillouin zone and spherical truncation of the Coulomb interaction to avoid silane-silane interactions. For the GW calculations, we used the BERKELEYGW [32] package. We used a dielectric matrix energy cutoff of 6 Ry. To converge the self-energy with respect to bands, we explicitly included states up to 6 Ry above the vacuum level and then added to it a static-remainder [33] term. The dynamical contributions to the self-energy were treated within a generalized plasmon pole model [2,34]. We performed all calculations at three supercell volumes in a simple-cubic lattice corresponding to lattice constants of 22.5, 25, and 30 a.u. All the results presented were extrapolated to the infinite volume limit.

Table I shows the calculated ionization potential and LUMO energies from different methods and experiment. In particular,

TABLE I. HOMO and LUMO quasiparticle energies of the silane molecule calculated with the present and other approaches. All values are in eV.

Starting	HOMO		LUMO	
mean field	MF	MF+G_0W_0	MF	MF+G_0W_0
LDA	− 8.53	− 12.55	− 0.48	0.82
LDA [9]	− 8.4	− 12.7	− 0.6	1.1
LDA [13]	− 8.42	− 12.67	− 0.50	0.63
Full-Σ [13]		− 12.66		− 0.42
Full-Σ [9]		− 12.7		0.3
od-COHSEX	− 14.36	− 12.49	− 0.01	− 0.01
sc-COHSEX	− 14.06	− 12.86	− 0.01	0.00
QMC [9]		− 12.6		0.2
Experiment [35]		− 12.6		

with the traditional diagonal only G_0W_0 method, the LUMO quasiparticle energies range from 0.6 to 1.1 eV. In the table, the full-Σ approach of Refs. [9] and [13] refers to the approach in which the full G_0W_0 matrix has been diagonalized. This full-Σ result (within the limitation of a small number of DFT eigenfunction expansion) would be the "exact" result that sc-COHSEX+GW and the od-COHSEX+GW approaches should be compared to. In the full-Σ approaches of Refs. [9,13], the LUMO quasiparticle energy is found to be nearly 1 eV lower than the corresponding diagonal G_0W_0 energies and in much better agreement with the quantum Monte Carlo (QMC) results. The results with our methods for the LUMO quasiparticle level agree well with the full-Σ and QMC numbers.

The HOMO (bottom panel) and LUMO (top panel) charge distributions within LDA and within our sc-COHSEX and od-COHSEX approaches are plotted in Fig. 2. As expected, all the HOMO wave functions show an exponential decay into the vacuum. Comparing the HOMO wave functions between the three methods, one can see that they do not change significantly even though the sc-COHSEX and od-COHSEX approaches overbind the HOMO mean-field level. This is consistent with the fact that after the GW correction to the mean field, the ionization potential (from Table I) does not change much in these approaches. The LUMO wave functions, on the other hand, change substantially between the three methods. Within LDA, the LUMO wave function decays exponentially into the vacuum region. This is because the LDA wave function is ∼0.5 eV below the vacuum level. The sc-COHSEX and od-COHSEX LUMO wave functions, on the other hand, are much more delocalized. This is consistent with the results shown in Table I, which show the LUMO mean-field energy within sc-COHSEX and od-COHSEX approaches to be ∼0 eV. The GW correction to these LUMO states is negligible.

To examine whether the quasiparticle wave functions within the three approaches are close to their mean-field counterparts, in Fig. 3(b) we plot the contribution to the second-order perturbation correction [24] to the LUMO quasiparticle energy, $E^{\rm QP}_{\rm LUMO}$, from $\Sigma_{GW}(E_{\rm LUMO}) - \Sigma_{\rm MF}$ (where MF stands for mean field) from intermediate states 1 to 40. The LDA mean-field ($\Sigma_{\rm MF} = V_{\rm XC}$) starting points from states 9, 15, 29, and 40 show large corrections to the quasiparticle energy. This corresponds to large off-diagonal elements in the Σ matrix in the Kohn-Sham orbital basis, which illustrates a failure of LDA to correctly describe the LUMO quasiparticle orbital. If one accounts for these second-order corrections, the LUMO quasiparticle energy becomes close to those from more accurate approaches. However, this comes at an additional cost of evaluating off-diagonal Σ matrix elements in the Kohn-Sham basis. It should be noted that in this case, expansion of the quasiparticle wave function in eigenstates within a few eV of the LUMO mean-field level is sufficient to get the correct result. However, the number of eigenstates in this energy range will depend on the size of the supercell. If the supercell is

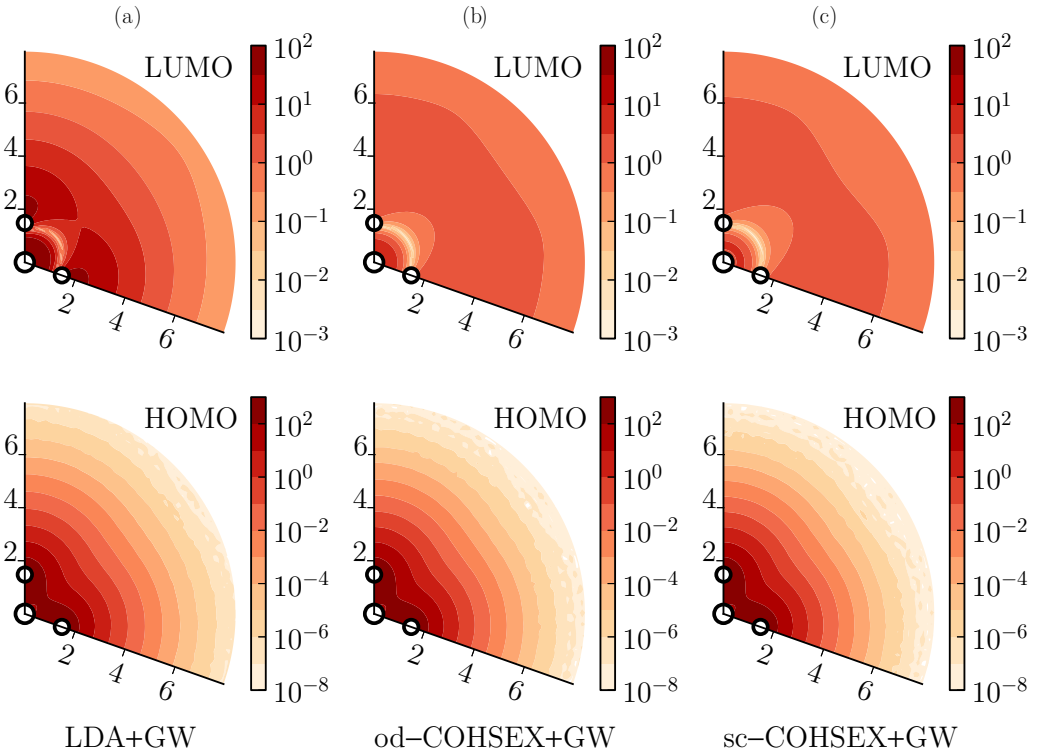

FIG. 2. (Color online) Polar contour plots of the modulus square of the quasiparticle wave function in a plane defined by Si (circle at the origin) and two H atoms (small circles along the radial direction). The radial direction in the plot is in Å, while the angle formed between the Si–H bonds is 109.47°. For the LUMO $|\psi_5(\mathbf{r})|^2$ is plotted, and for the HOMO $\sum_{n=2,3,4}|\psi_n(\mathbf{r})|^2$ is plotted. The HOMO (bottom panels) and LUMO (top panels) quasiparticle wave functions of the silane molecule are within (a) LDA+GW, (b) od-COHSEX+GW, and (c) sc-COHSEX+GW.

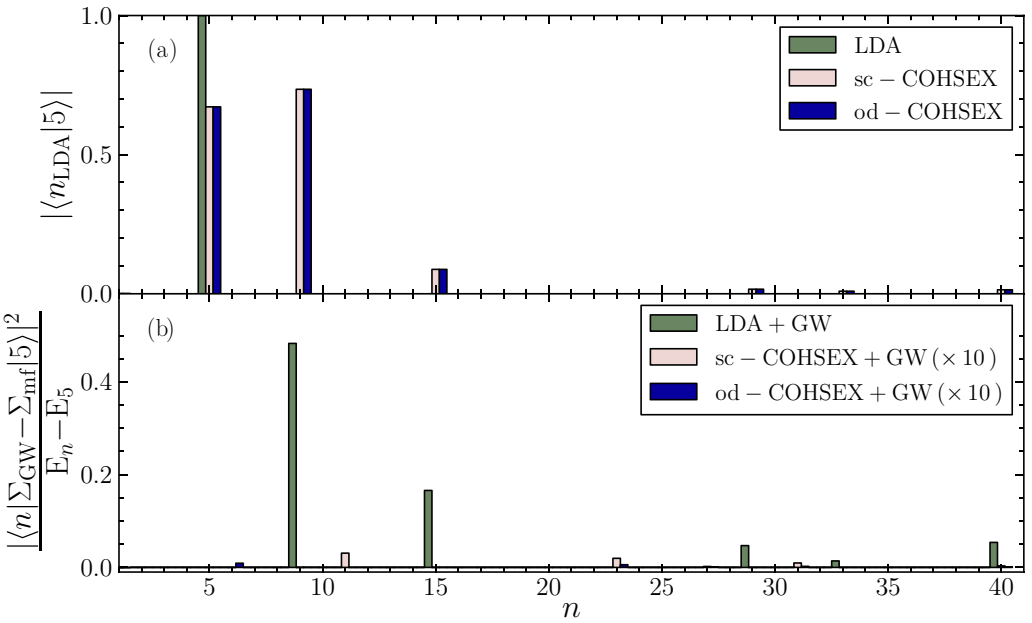

FIG. 3. (Color online) The top panel shows the overlap $|\langle n_{\rm LDA}|5\rangle|$ vs n in silane within the LDA, sc-COHSEX, and od-COHSEX approaches. The bottom panel shows the contributions (in eV) to the second-order perturbation correction from each state n to the quasiparticle energy of the LUMO, state 5, in silane within the LDA+GW, sc-COHSEX+GW, and od-COHSEX+GW approaches. As indicated in the legend, the corrections in the latter two approaches are multiplied by a factor of 10 for clarity.

much larger, this number can become quite large, making the calculation much more expensive. Furthermore, predicting this energy range is also not straightforward. Also seen in Fig. 3(b), the contributions in both the sc-COHSEX+GW approach and the od-COHSEX+GW approach are small. In both new approaches, the off-diagonal elements of Σ in the new COHSEX orbital basis are small and are effectively included in the mean-field starting point (sc-COHSEX) or treated adequately within the static approximation (od-COHSEX approach). This means that the quasiparticle wave functions are well described by the sc-COHSEX and od-COHSEX wave functions, respectively. We analyzed the LUMO mean-field wave function within od-COHSEX and sc-COHSEX in terms of the LDA wave functions in order to examine the difference in the LUMO quasiparticle wave functions within the three methods. Figure 3(a) shows the overlap between the new mean-field LUMO wave functions and LDA wave functions. As can be seen in Fig. 3(a), the major contributions to the od-COHSEX and sc-COHSEX LUMO wave functions come from the 5, 9, 15, 29, 33, and 40 LDA states. These are the states within the LDA mean field that possess significant off-diagonal matrix elements. This indicates that the od-COHSEX and sc-COHSEX methods mix these orbitals appropriately to construct the LUMO quasiparticle wave function such that the self-energy operator is diagonal in this basis.

We now turn our attention to an example of a failure of the mean-field band structure. An example for this case is bulk Ge. It is well known that within the LDA [8], the direct band gap of bulk Ge can be negative, i.e., bulk Ge is often predicted to be a metal within DFT while experimentally it is a well-known semiconductor. This is a qualitative failure of the mean-field band structure. With care, GW is known to resolve this problem [2,8]; however, often this is done by iterating the eigenvalues used to construct G and W. We studied bulk Ge under negative hydrostatic pressure. The pressure coefficients of various band gaps of bulk Ge have been calculated [38–41] and measured [36,37]. As one applies a negative hydrostatic pressure on Ge, the band gaps are expected to become smaller and the failure of the LDA Kohn-Sham gap more severe. We performed our calculations at $P = -3.5$ GPa. These calculations were done with an $8 \times 8 \times 8$ k-point sampling of the Brillouin zone, a 40 Ry cutoff for the wave functions, and an 8 Ry cutoff for the dielectric matrix. The generalized plasmon pole model [2,34] was used to extend the static dielectric matrix to finite frequencies. It should be noted that we used a pseudopotential containing nonlinear core correction to determine the structural properties and pressure. However, we used a pseudopotential without any nonlinear core correction as a mean-field starting point for the GW calculation. This is because there is no obvious way to generalize the nonlinear core correction to GW calculations as the self-energy operator in GW calculations does not explicitly depend on the charge density. As the partial core charge density is built into the pseudopotential, its use in $V_{\rm XC}$ term of Eq. (2) may lead to erroneous results. For this reason, and more importantly the fact that the exchange interaction with the semicore states is significant, it is well known and standard practice in GW calculations to take the semicore states (of the same principal quantum number as the valence states) as explicit states in the pseudopotential generation. To calculate the dielectric matrix at $\mathbf{q} = \mathbf{0}$, a $100 \times 100 \times 100$ k-point sampling was used in the LDA where bulk Ge was found to be a metal.

Table II shows the results of our calculation on bulk Ge at $P = -3.5$ GPa. As can be seen from the table, the Γ-Γ gap within the LDA is negative. This is due to the well-known band inversion at the Γ point. However, when one performs a

TABLE II. Direct gap at Γ and indirect band gap (Γ-L) for bulk Ge at $P = -3.5$ GPa calculated within various approximations. All values are in eV.

		Γ-Γ		Γ-L	
Iter	Mean field	MF	MF+G_0W_0	MF	MF+G_0W_0
0	LDA	–0.38	–0.15	0.00	0.44
1	sc-COHSEX+GW	0.64	0.45	1.07	0.77
2	sc-COHSEX+GW	0.54	0.50	0.97	0.80
3	sc-COHSEX+GW	0.57	0.51	0.99	0.80
	Experiment [36,37]		0.35		0.6

one-shot diagonal G_0W_0 calculation with parameters mentioned above, there is still no band gap opening. It is conceivable that iterating G and W with updated eigenvalues may open a band gap in such a case—however, a band gap opening should correspond to qualitative changes in the spatial dependence of G and W as well. Simple eigenvalue iteration within the diagonal approximation would completely miss such a spatial dependence change. Similarly, the od-COHSEX+GW approach also does not open the band gap. This is because the od-COHSEX does not change the DFT mean-field starting point of the GW calculation. The first iteration of sc-COHSEX opens up a gap, and the ordering of the levels at the Γ point becomes correct. Similarly, at the L point, the mean-field LDA has a zero gap, while in the first iteration of sc-COHSEX, a gap opens up. Subsequent iterations only change the result quantitatively—with two iterations sufficient to get convergence. It should be noted that our results in Table II are without any spin-orbit correction, while the experimental band gap includes this effect. As mentioned earlier, in the absence of vertex corrections and electron-phonon renormalization, it is expected that sc-COHSEX+GW would overestimate band gaps.

Table III shows the result of application of these approaches to bulk Si. These calculations were done with a $6 \times 6 \times 6$ k-point sampling of the Brillouin zone, a 35 Ry cutoff for the wave functions, and a 12 Ry cutoff for the dielectric matrix. The generalized plasmon pole model [2,34] was used to extend the static dielectric matrix to finite frequencies. Table III shows our calculated values of the direct and indirect band gaps in silicon. As can be seen in the table, the od-COHSEX+GW approach gives the same gaps as previous

TABLE III. Direct gap at Γ and indirect band gap for silicon calculated within various approximations. All values are in eV.

	Direct gap		Fundamental gap	
Mean field	MF	MF+G_0W_0	MF	MF+G_0W_0
LDA	2.56	3.29	0.53	1.29
LDA [2]	2.57	3.35	0.52	1.29
LDA [12]	2.57	3.20	0.51	1.14
sc-COHSEX+GW [12]		3.69		1.56
od-COHSEX+GW	3.79	3.32	1.82	1.29
sc-COHSEX+GW	3.74	3.69	1.72	1.63
Experiment [37]		3.40		1.17

calculations using the diagonal Σ approximation within the Kohn-Sham basis [2]. Our approach agrees with previous sc-COHSEX [12] approaches. However, both overestimate the gaps slightly due to the aforementioned reasons.

VI. CONCLUSION

In summary, we present two approaches for going beyond the diagonal Σ constructed within G_0W_0 and the DFT mean field. Both approaches construct the quasiparticle Hamiltonian in the static approximation of GW within a plane-wave basis and diagonalize it. The sc-COHSEX+GW approach can be viewed as a diagonal G_0W_0 approach with improved mean-field starting orbitals and energies where the off-diagonal matrix elements of Σ-Σ_{MF} are small. The od-COHSEX+GW approach does not change the mean-field starting point of a typical DFT+GW calculation, but it constructs a new basis of COHSEX orbitals in which the off-diagonal matrix elements of Σ-Σ_{DFT} are small. We show that both methods give good quasiparticle wave functions and energies for the molecular states of silane (in particular the LUMO), and that with both approaches the off-diagonal elements of Σ in the COHSEX orbital basis are small. Further, the sc-COHSEX+GW method gives an alternate mean-field starting point for GW calculations. In the case of bulk Ge under pressure, we find that sc-COHSEX+GW fixes a failure of the LDA band structure by correctly predicting a semiconducting band structure. In bulk Si, od-COHSEX+GW gives band gaps in good agreement with experiment and previous calculations, while sc-COHSEX+GW slightly overestimates them as in other self-consistent GW methods.

ACKNOWLEDGMENTS

This research was supported by the SciDAC Program on Excited State Phenomena in Energy Materials funded by the U.S. Department of Energy, Office of Basic Energy Sciences and of Advanced Scientific Computing Research, under Contract No. DE-AC02-05CH11231 at Lawrence Berkeley National Laboratory and under Award No. DE-SC0008877 at the University of Texas, Austin, which provided for algorithm and code developments and simulations; and by the National Science Foundation under Grant No. DMR10-1006184, which provided for the basic theory and formalism. S.G.L. acknowledges the support of a Simons Foundation Fellowship in Theoretical Physics. M.L.C. acknowledges support by the Theory Program funded by the U.S. Department of Energy, Basic Energy Sciences, under Contract No. DE-AC02-05CH11231. In this research, use was made of resources of the National Energy Research Scientific Computing Center, which is supported by the Office of Science of the U.S. Department of Energy.

APPENDIX: USE OF SYMMETRY

Using symmetries of the crystal and the atoms, the calculation can be reduced to getting eigenvalues and eigenfunctions at $\mathbf{k}$ in the irreducible part of the Brillouin zone. However, for evaluating $\Sigma_{\mathrm{COHSEX}}\psi$, wave functions in the full Brillouin zone are required. To construct the wave functions in the full

Brillouin zone from those in the reduced Brillouin zone, the following relation for constructing the cell periodic part of the wave function, $u_{n,\mathbf{k}'}(\mathbf{G})$ at $\mathbf{k}' = \mathbf{R}(\mathbf{k})$, can be used:

$$u_{n,\mathbf{R}(\mathbf{k})}(\mathbf{G}) = u_{n,\mathbf{k}}[\mathbf{R}^{-1}(\mathbf{G})]e^{-i\mathbf{G}\cdot\tau}, \tag{A1}$$

where the symmetry operation is defined by a reciprocal-space rotation matrix $\mathbf{R}$ and a fractional translation τ such that $\mathbf{r}' = \mathbf{R}^{-1}\mathbf{r} + \tau$. Similarly, one can construct the screened Coulomb interaction at a $\mathbf{q}_1$ defined as $\mathbf{q}_1 = \mathbf{R}(\mathbf{q}) + \mathbf{G}_R$, where $\mathbf{G}_R$ is a $\mathbf{G}$-vector chosen to ensure that $\mathbf{q}$ and $\mathbf{q}_1$ are in the first Brillouin zone. Then one can use the relation [2,42]

$$\epsilon^{-1}_{\mathbf{q}_1}(\mathbf{G},\mathbf{G}') = e^{-i(\mathbf{G}-\mathbf{G}')\cdot\tau}\epsilon^{-1}_{\mathbf{q}}(\mathbf{G}_1\mathbf{G}'_1), \tag{A2}$$

where $\mathbf{G}_1 = \mathbf{R}^{-1}(\mathbf{G} + \mathbf{G}_R)$.

[1] L. Hedin and S. Lundqvist, in *Advances in Research and Applications*, Solid State Physics Vol. 23, edited by F. Seitz, D. Turnbull, and H. Ehrenreich (Academic, New York, 1970), pp. 1–181.

[2] M. S. Hybertsen and S. G. Louie, Phys. Rev. Lett. **55**, 1418 (1985); Phys. Rev. B **34**, 5390 (1986).

[3] R. W. Godby, M. Schlüter, and L. J. Sham, Phys. Rev. B **37**, 10159 (1988).

[4] J. E. Northrup, M. S. Hybertsen, and S. G. Louie, Phys. Rev. Lett. **59**, 819 (1987); Phys. Rev. B **39**, 8198 (1989).

[5] C. D. Spataru, S. Ismail-Beigi, L. X. Benedict, and S. G. Louie, Phys. Rev. Lett. **92**, 077402 (2004); J. Deslippe, C. D. Spataru, D. Prendergast, and S. G. Louie, Nano Lett. **7**, 1626 (2007).

[6] V. I. Anisimov, J. Zaanen, and O. K. Andersen, Phys. Rev. B **44**, 943 (1991).

[7] M. Gatti, F. Bruneval, V. Olevano, and L. Reining, Phys. Rev. Lett. **99**, 266402 (2007).

[8] E. L. Shirley, X. Zhu, and S. G. Louie, Phys. Rev. B **56**, 6648 (1997).

[9] J. C. Grossman, M. Rohlfing, L. Mitas, S. G. Louie, and M. L. Cohen, Phys. Rev. Lett. **86**, 472 (2001).

[10] A. Janotti, J. B. Varley, P. Rinke, N. Umezawa, G. Kresse, and C. G. Van de Walle, Phys. Rev. B **81**, 085212 (2010); A. Malashevich, M. Jain, and S. G. Louie, *ibid.* **89**, 075205 (2014).

[11] S. V. Faleev, M. van Schilfgaarde, and T. Kotani, Phys. Rev. Lett. **93**, 126406 (2004).

[12] F. Bruneval, N. Vast, and L. Reining, Phys. Rev. B **74**, 045102 (2006).

[13] P. H. Hahn, W. G. Schmidt, and F. Bechstedt, Phys. Rev. B **72**, 245425 (2005).

[14] F. Fuchs, J. Furthmüller, F. Bechstedt, M. Shishkin, and G. Kresse, Phys. Rev. B **76**, 115109 (2007).

[15] V. I. Anisimov, F. Aryasetiawan, and A. I. Lichtenstein, J. Phys.: Condens. Matter **9**, 767 (1997).

[16] T. Körzdörfer and N. Marom, Phys. Rev. B **86**, 041110 (2012).

[17] H. Jiang, R. I. Gomez-Abal, P. Rinke, and M. Scheffler, Phys. Rev. B **82**, 045108 (2010).

[18] B.-C. Shih, T. A. Abtew, X. Yuan, W. Zhang, and P. Zhang, Phys. Rev. B **86**, 165124 (2012).

[19] A. Seidl, A. Görling, P. Vogl, J. A. Majewski, and M. Levy, Phys. Rev. B **53**, 3764 (1996).

[20] T. Stein, H. Eisenberg, L. Kronik, and R. Baer, Phys. Rev. Lett. **105**, 266802 (2010).

[21] S. Refaely-Abramson, R. Baer, and L. Kronik, Phys. Rev. B **84**, 075144 (2011).

[22] M. Jain, J. R. Chelikowsky, and S. G. Louie, Phys. Rev. Lett. **107**, 216806 (2011).

[23] T. Körzdörfer, R. M. Parrish, N. Marom, J. S. Sears, C. D. Sherrill, and J.-L. Brédas, Phys. Rev. B **86**, 205110 (2012).

[24] J.-L. Li, G.-M. Rignanese, E. K. Chang, X. Blase, and S. G. Louie, Phys. Rev. B **66**, 035102 (2002).

[25] W. Kohn and L. J. Sham, Phys. Rev. **140**, A1133 (1965).

[26] J. P. Perdew, K. Burke, and M. Ernzerhof, Phys. Rev. Lett. **77**, 3865 (1996).

[27] M. Rohlfing and S. G. Louie, Phys. Rev. B **62**, 4927 (2000).

[28] B. Holm and U. von Barth, Phys. Rev. B **57**, 2108 (1998).

[29] F. Aryasetiawan, L. Hedin, and K. Karlsson, Phys. Rev. Lett. **77**, 2268 (1996).

[30] M. L. Cohen, M. Schlüter, J. R. Chelikowsky, and S. G. Louie, Phys. Rev. B **12**, 5575 (1975).

[31] http://www.nersc.gov/projects/paratec/.

[32] J. Deslippe, G. Samsonidze, D. Strubbe, M. Jain, M. L. Cohen, and S. G. Louie, Comput. Phys. Commun. **183**, 1269 (2012).

[33] J. Deslippe, G. Samsonidze, M. Jain, M. L. Cohen, and S. G. Louie, Phys. Rev. B **87**, 165124 (2013).

[34] S. B. Zhang, D. Tománek, M. L. Cohen, S. G. Louie, and M. S. Hybertsen, Phys. Rev. B **40**, 3162 (1989).

[35] U. Itoh, Y. Toyoshima, H. Onuki, N. Washida, and T. Ibuki, J. Chem. Phys. **85**, 4867 (1986).

[36] A. R. Goñi, K. Syassen, and M. Cardona, Phys. Rev. B **39**, 12921 (1989).

[37] Landolt-Börnstein, *Numerical Data and Functional Relationships in Science and Technology*, New Series Group III, Vol. 17, Pt A. (Springer, New York, 1982).

[38] D. L. Camphausen, G. A. N. Connell, and W. Paul, Phys. Rev. Lett. **26**, 184 (1971).

[39] K. Chang, S. Froyen, and M. L. Cohen, Solid State Commun. **50**, 105 (1984).

[40] E. Ghahramani and J. E. Sipe, Phys. Rev. B **40**, 12516 (1989).

[41] P. Modak, A. Svane, N. E. Christensen, T. Kotani, and M. van Schilfgaarde, Phys. Rev. B **79**, 153203 (2009).

[42] M. S. Hybertsen and S. G. Louie, Phys. Rev. B **35**, 5585 (1987).